SUPPORTING FIGURES

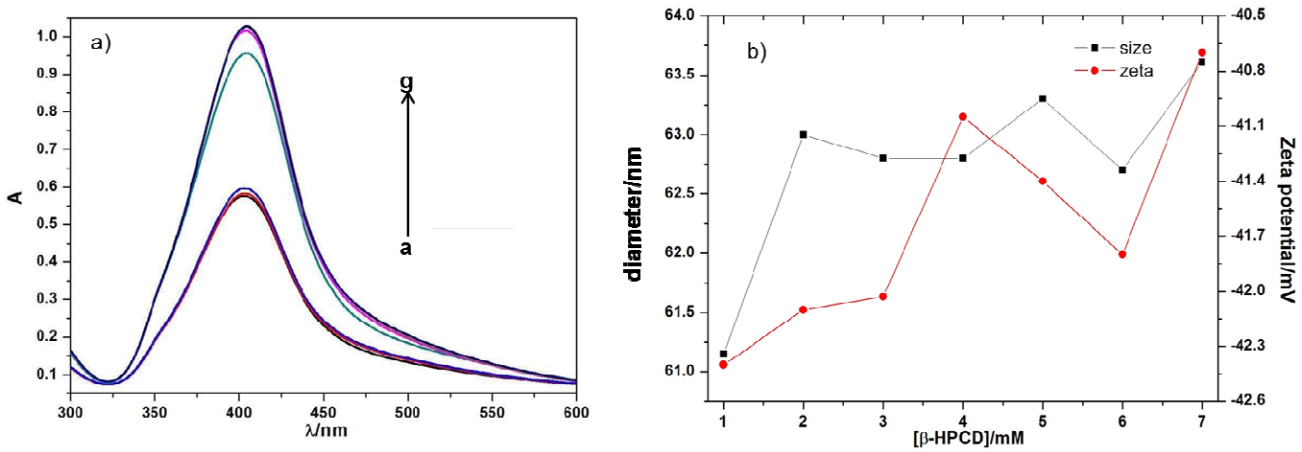

Figure S1. (a) UV-vis spectra and (b) DLS analysis for the formation of AgNPs at various time intervals in the presence of β – HPCD. Curves (a-g): 1, 2, 3, 4, 5, 6, and 7 h

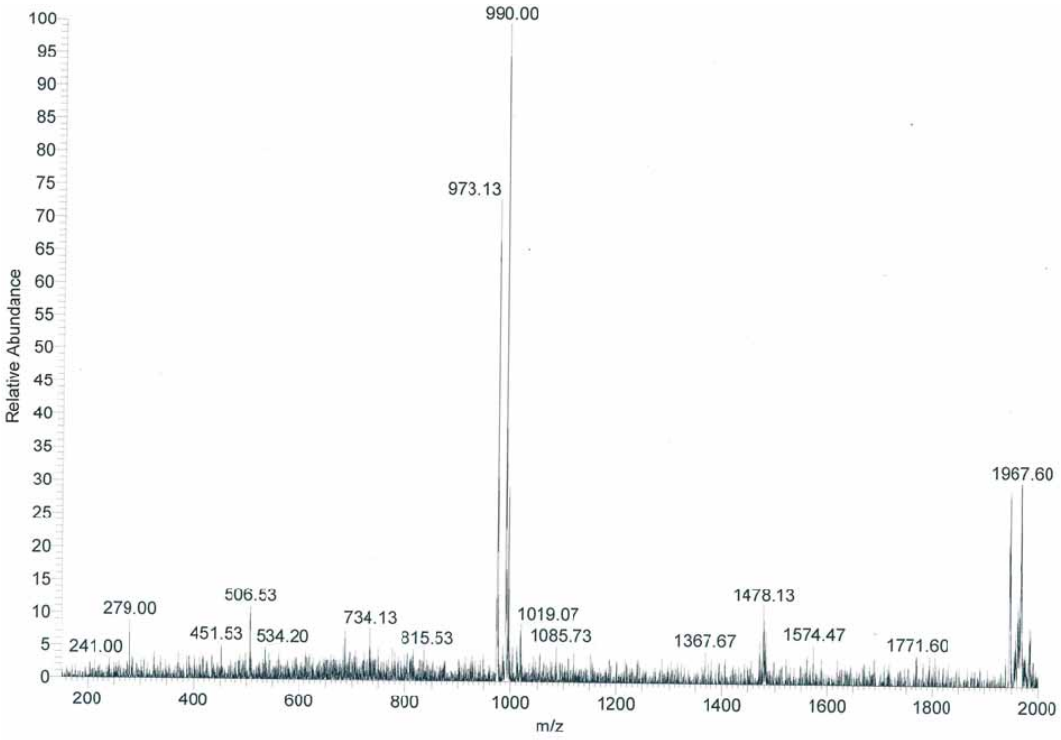

Figure S2. Mass spectra of α-CD

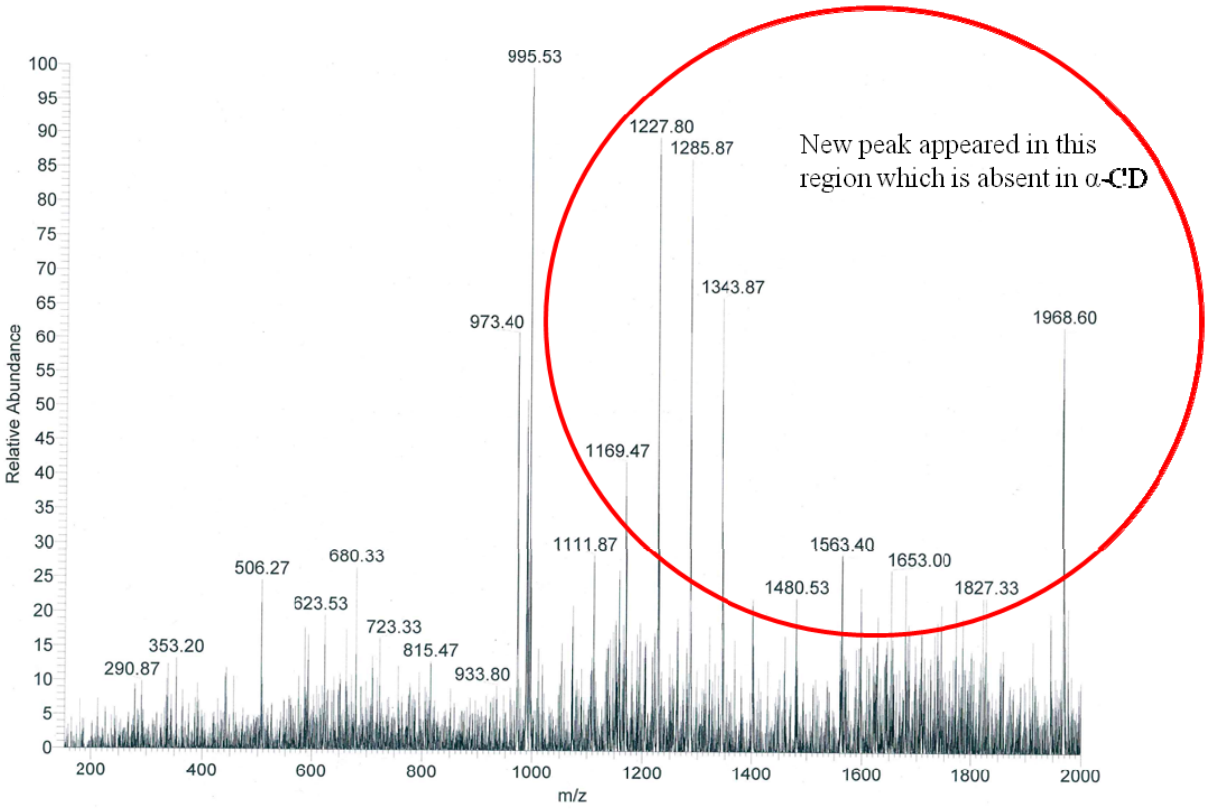

Figure S3. Mass spectra of α-CD-AgNPs

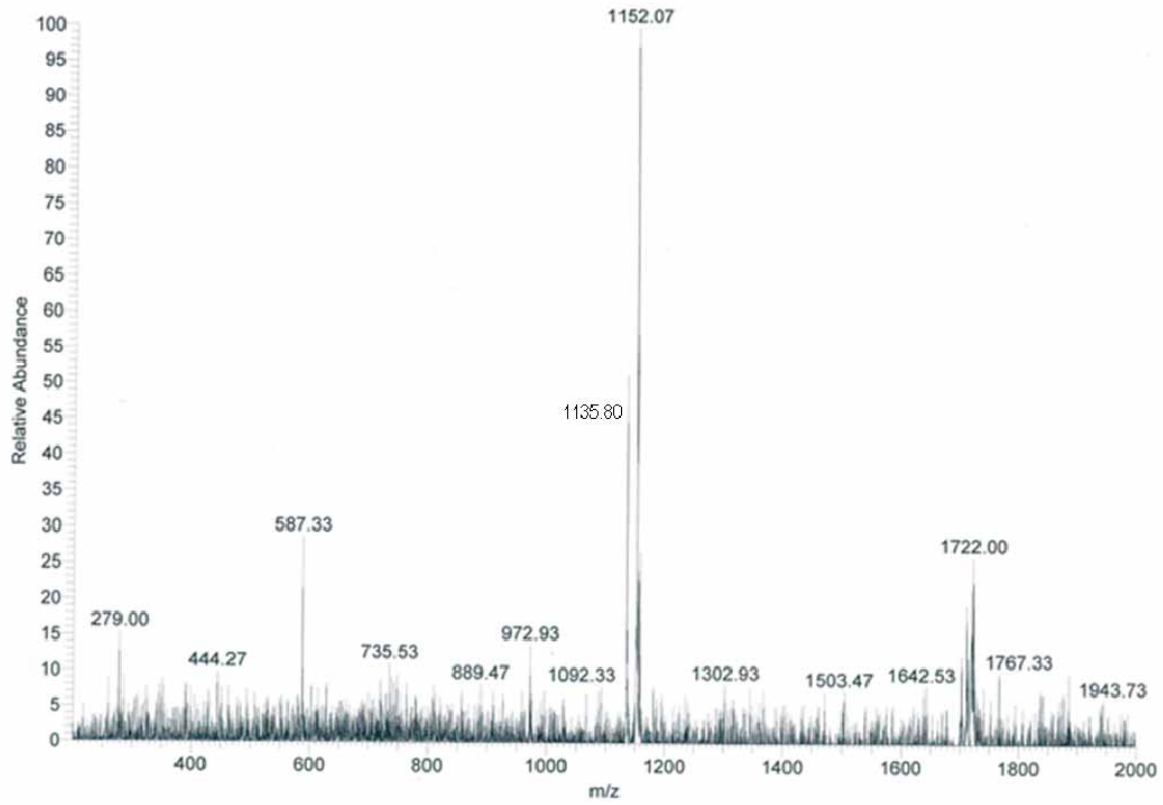

Figure S4. Mass spectra of β-CD

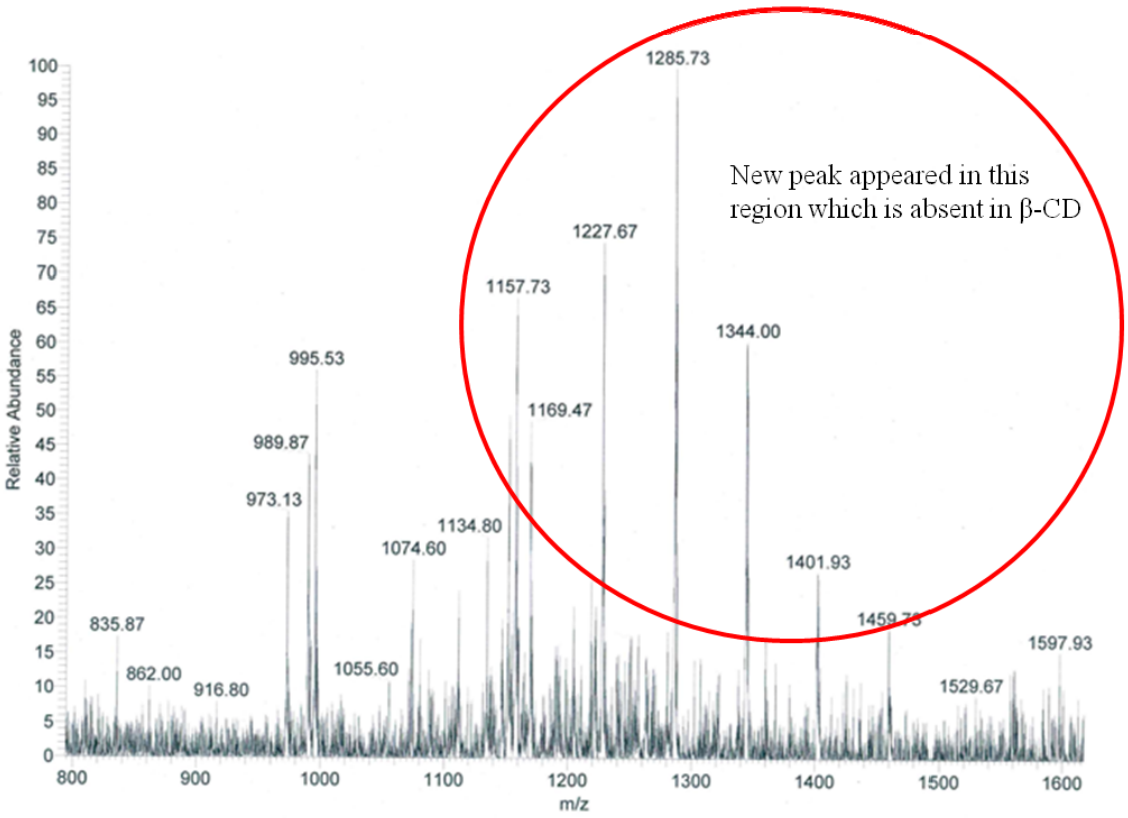

Figure S5. Mass spectra of β-CD-AgNPs

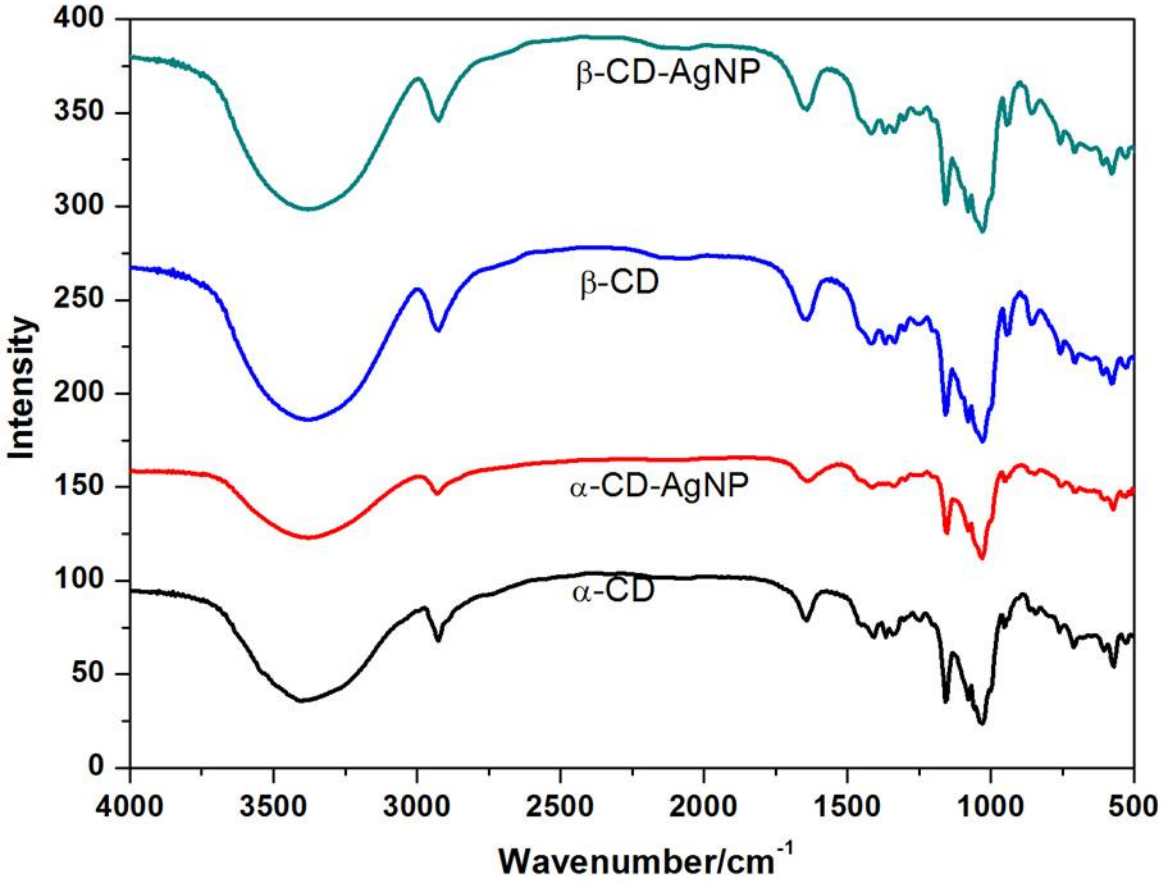

Figure S6. FT-IR spectra of CD and CD-AgNPs

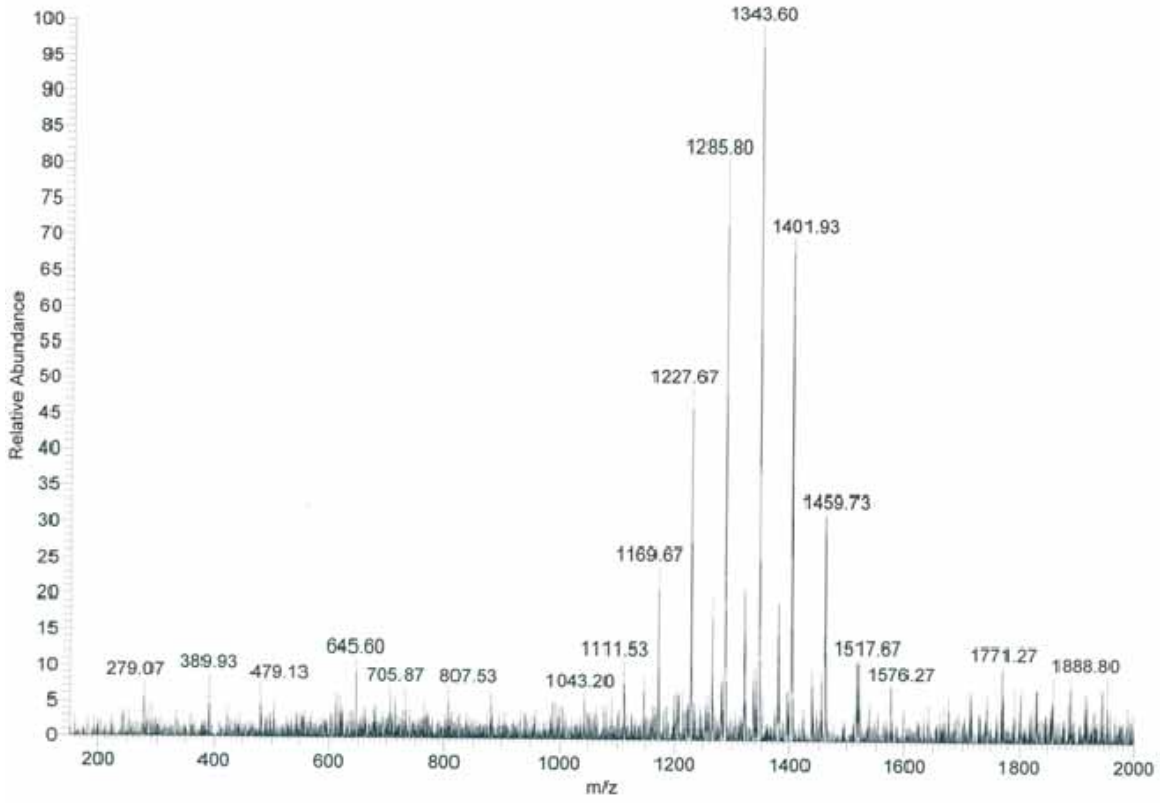

Figure S7. Mass spectra of α-HPCD

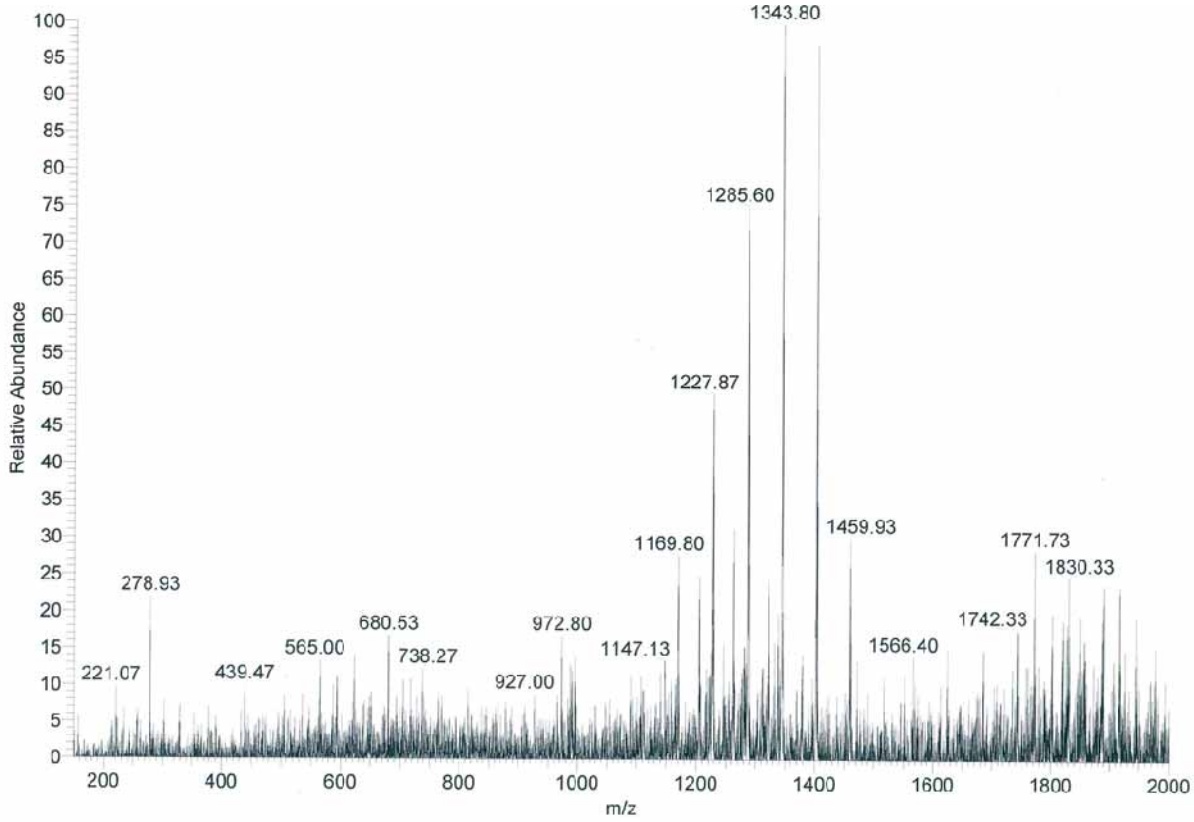

Figure S8. Mass spectra of α-HPCD-AgNPs

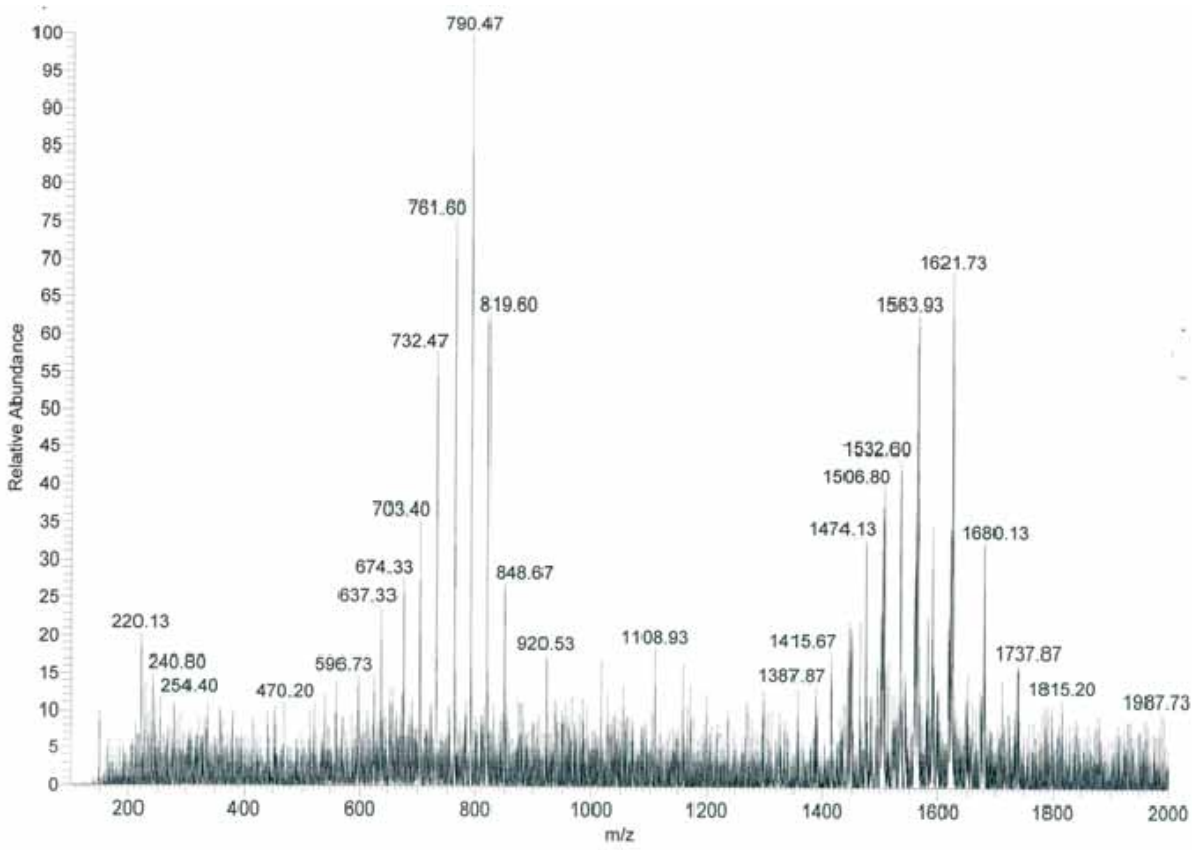

Figure S9. Mass spectra of β-HPCD

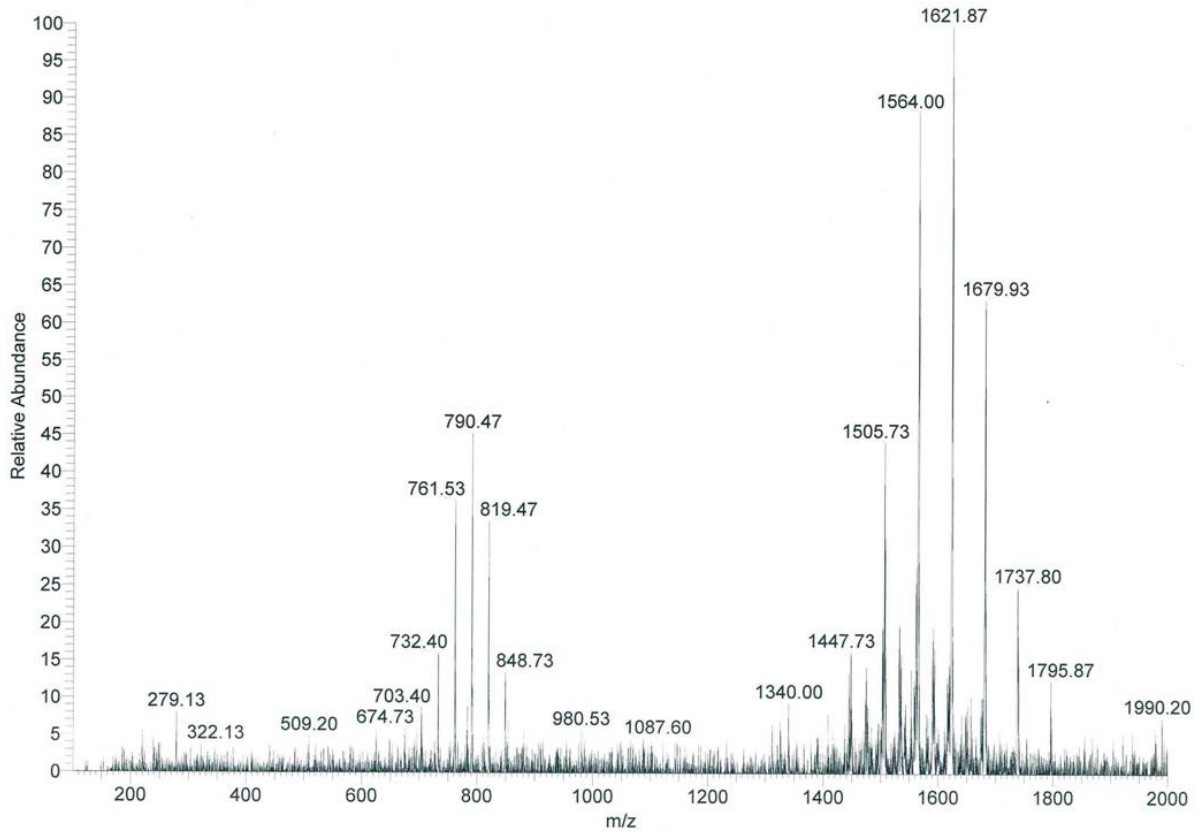

Figure S10. Mass spectra of β-HPCD-AgNPs

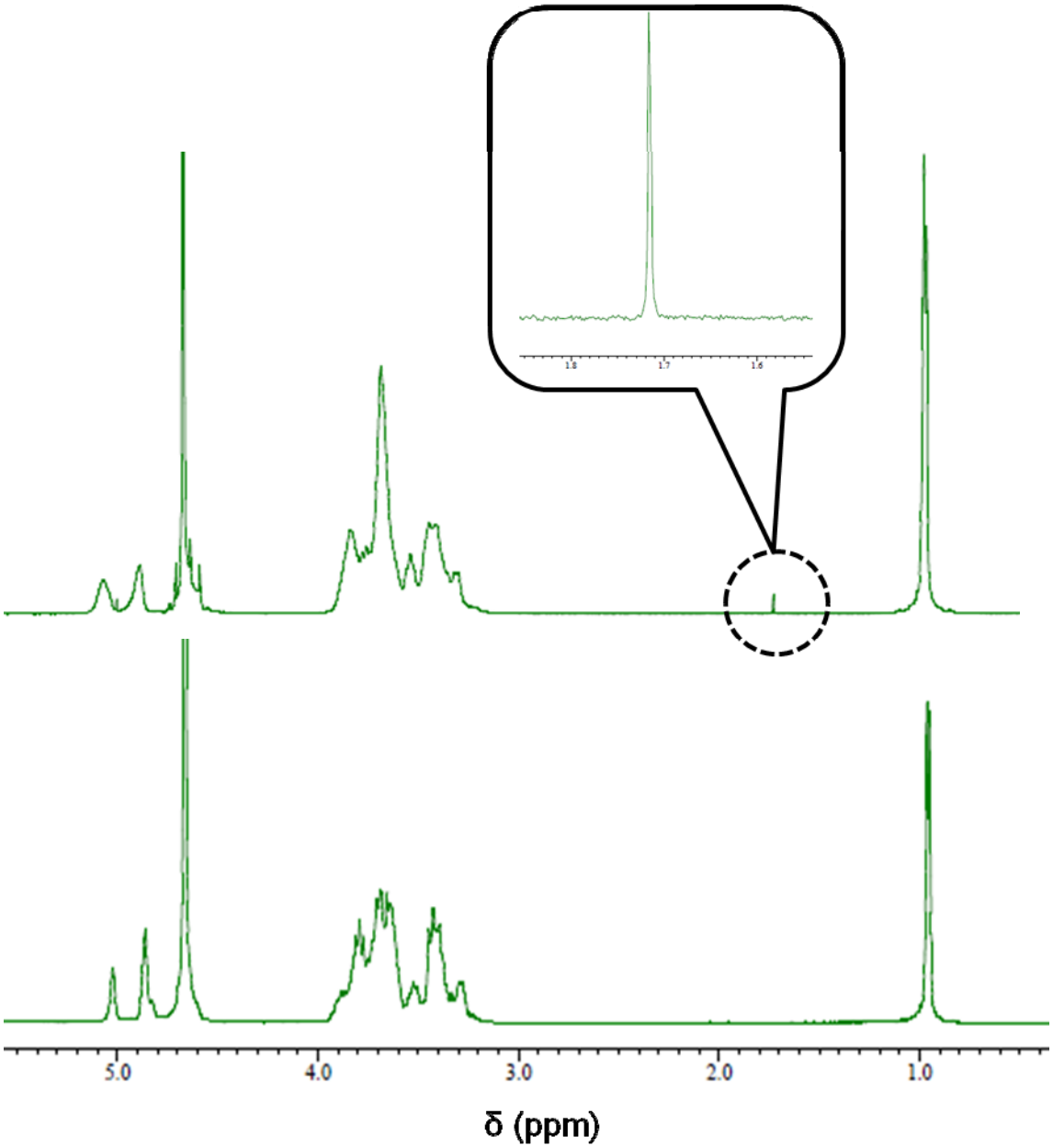

Figure S11. ^{1}H NMR spectra (400 MHz, 25℃) in D_2O a) β-HPCD and b) β -HPCD-AgNPs. Inset was taken from the spectral regions shown by the dotted circles

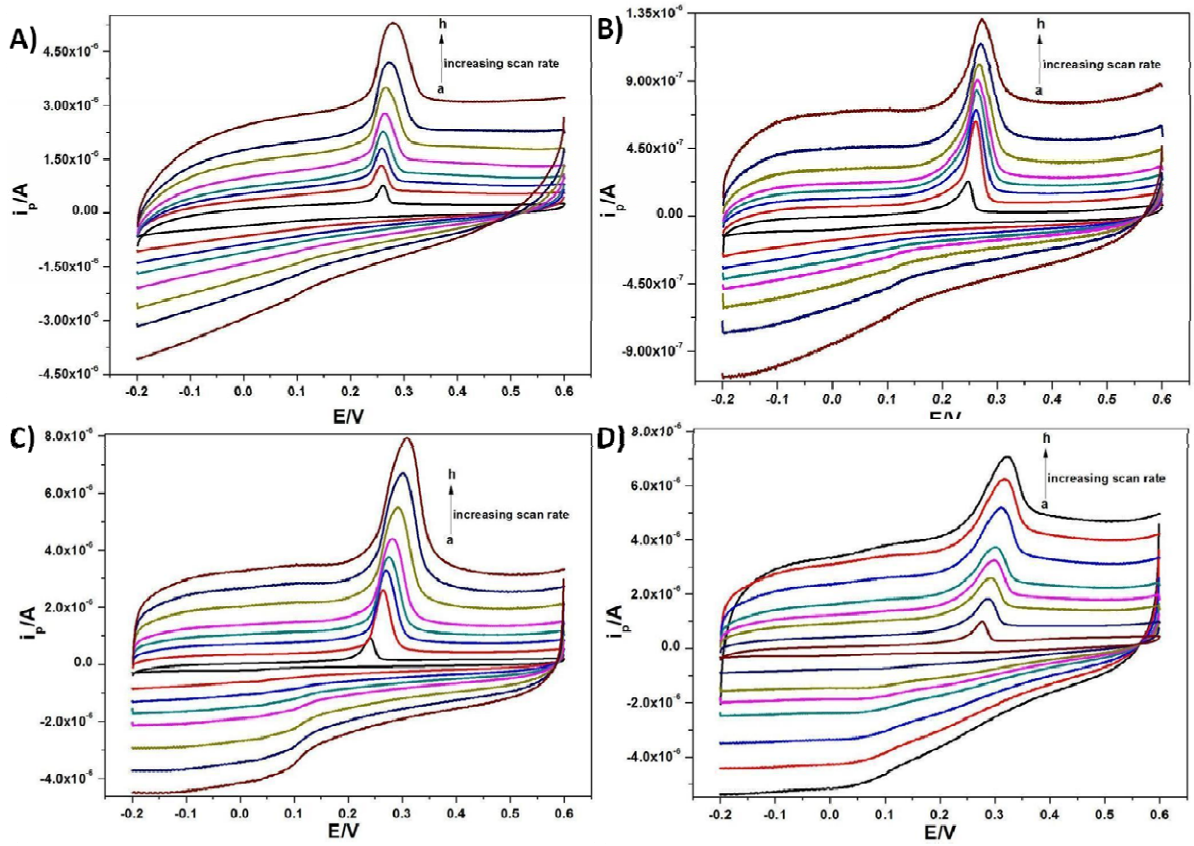

Figure S12. Cyclic Voltammogram of A) α – CD -AgNPs; B) β – CD-AgNPs; C) β – HPCD-AgNPs; and D) α – HPCD-AgNPs at different scan rate : (a) 10, (b) 50, (c) 100, (d) 150, (e) 200, (f) 300, (g) 400, and (h) 500 mV s^{-1} in 0.01M PB using Glassy carbon as working electrode, Pt wire as counter and SCE as reference.

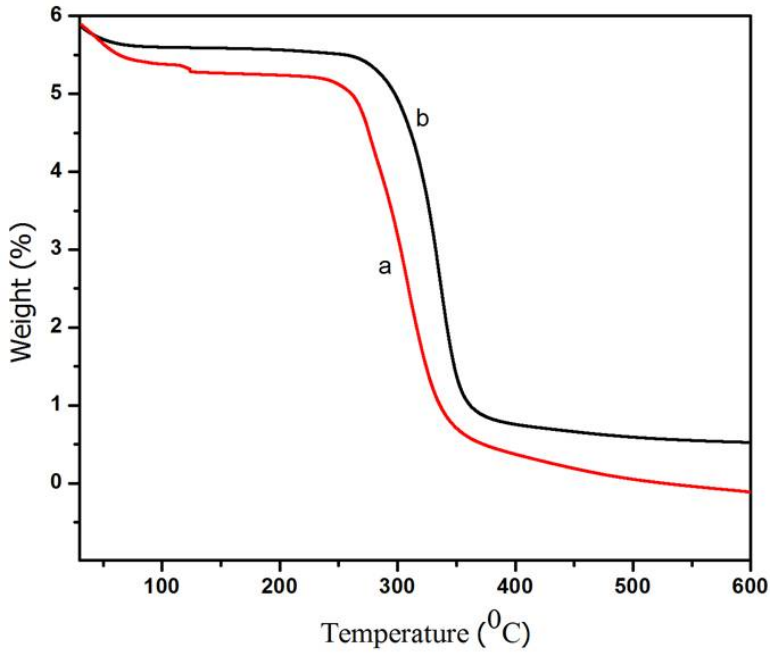

Figure S13. TGA of β-HPCD (curve a) and β-HPCD-AgNP (curve b)

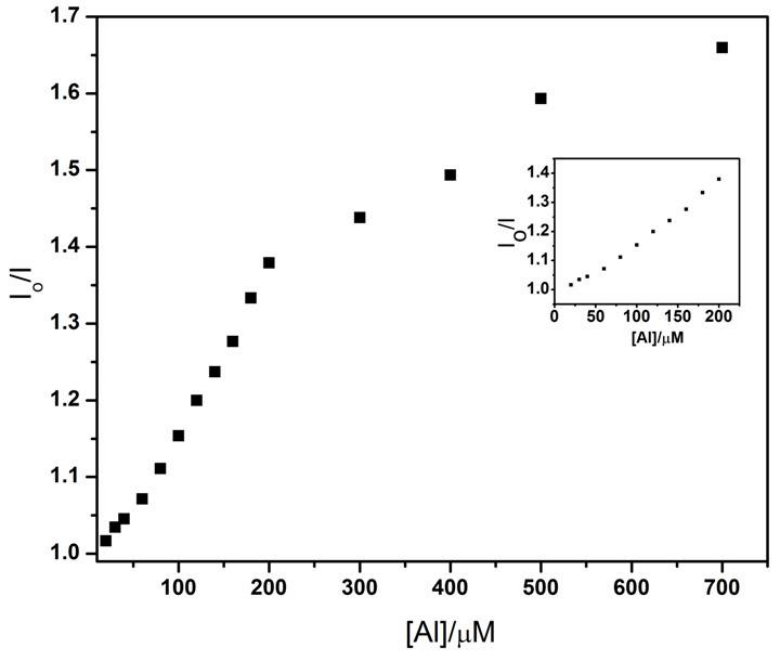

Figure S14. Stern-Volmer plot of I_o/I against [Al(III)]. The inset displays the linear relationship of the Stern-Volmer plot at the low concentration range (20-200 μM) of Al(III). I_o and I are the PL intensities of β-HPCD-AgNP at excitation/emission wavelengths of 400/540 nm in the absence and presence of Al(III), respectively

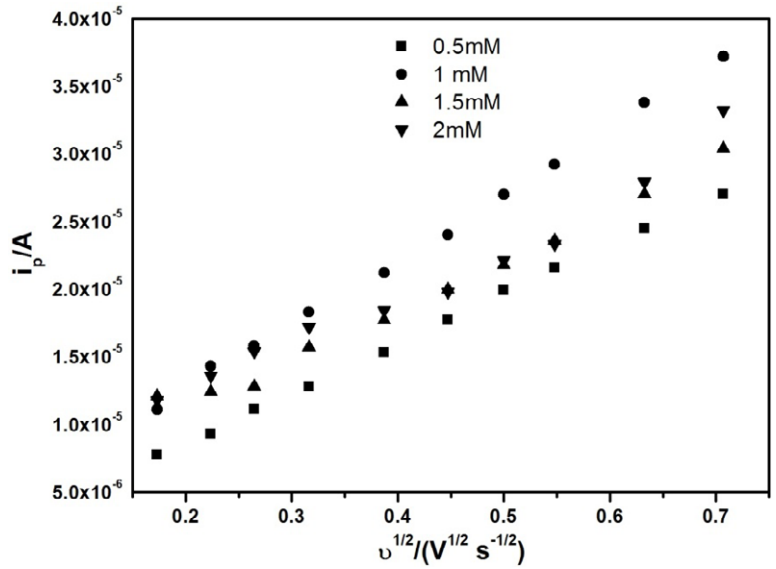

Figure S15. Plot of peak current (i_p) versus square root of scan rate ($\sqrt{\nu}$) for the catalytic reduction of PNP over GC/β-HPCD-AgNP: [PNP] = 0.5mM, [β-HPCD-AgNPs]; ■ = 0.5, ●= 1, ▲= 1.5, and ▼= 2 mM, respectively.

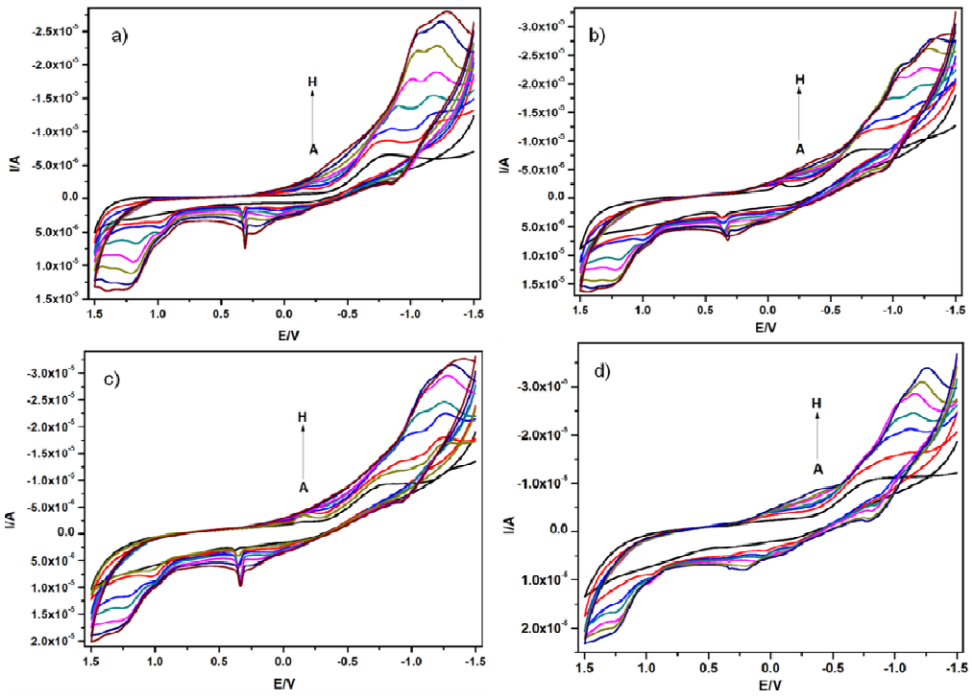

Figure S16. CV of β-HPCD-AgNP a) 0.05, b) 0.1, c) 0.15, and d) 0.2 mM in the presence of various concentration of PNP: A) 0, B) 0.05, C) 0.1, D) 0.2, E) 0.3, F) 0.4, G) 0.5, and H) 0.6 mM. Scan rate 100mV/s.

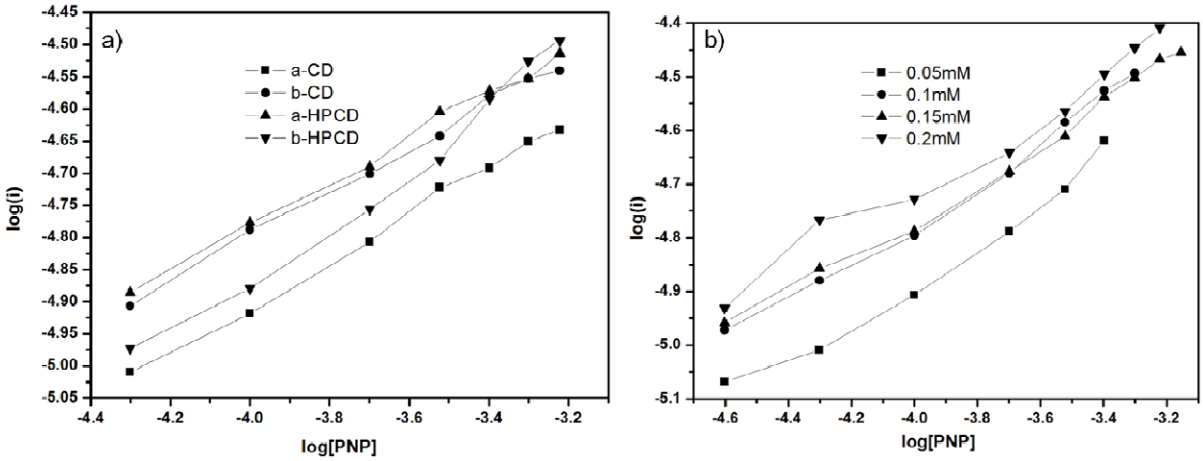

Figure S17. Plot of log(i) versus log[PNP]. a) Different CD capped AgNPs and b) Different concentration of β-HPCD capped AgNPs